Mercury Sources and Fate in a Large Brackish Ecosystem (the Baltic Sea) Depicted by Stable Isotopes

Sylvain Bouchet, Anne Soerensen, Erik Björn, Emmanuel Tessier, David Amouroux

Mercury sources and fate in a large brackish ecosystem (the Baltic Sea) depicted by stable isotopes

Sylvain Bouchet[1†*], Anne L. Soerensen[2], Erik Björn[3], Emmanuel Tessier[1], David Amouroux[1]

[1] Université de Pau et des Pays de l'Adour, E2S UPPA, CNRS, IPREM, Institut des Sciences Analytiques et de Physico-Chimie pour l'Environnement et les Matériaux, 64 000 Pau, France

[2] Swedish Museum of Natural History, Department of Environmental Research and Monitoring, 104 05 Stockholm, Sweden

[3] Umeå University, Department of Chemistry, 90187, 901 87 Umeå, Sweden

[†]Present address: ETH Zürich, D-USYS department, Universitätstrasse 16, 8092 Zürich, Switzerland

*Corresponding author: sylvain.bouchet@usys.ethz.ch; Phone: +41 44 633 60 24

ABSTRACT

Identifying Hg sources to aquatic ecosystems and processes controlling the levels of monomethylmercury (MMHg) is critical for developing efficient policies of Hg emissions reduction. Here we measured Hg concentrations and stable isotopes in sediment, seston and fishes from the various basins of the Baltic Sea, a large brackish ecosystem presenting extensive gradients in salinity, redox conditions, dissolved organic matter (DOM) composition and biological activities. We found that Hg mass dependent fractionation (Hg-MDF) values in sediments mostly reflect a mixing between light terrestrial Hg and heavier industrial sources whereas odd Hg isotope mass independent fractionation (odd Hg-MIF) reveals atmospheric inputs. Seston presents intermediate Hg-MDF and odd Hg-MIF values falling between sediments and fish but in the north, high even Hg-MIF values suggests the preferential accumulation of wet-deposited Hg. Odd Hg-MIF values in fish indicate an overall low extent of MMHg photodegradation due to limited sunlight exposure and penetration, but also reveals large spatial differences. The photodegradation extent is lowest in the central basin with recurrent algal blooms due to their shading effect and highest in the northern, least saline basin with high concentrations of terrestrial DOM. As increased loads of terrestrial DOM are expected in many coastal areas due to global changes, its impact on MMHg photodegradation needs to be better understood and accounted for when predicting future MMHg concentrations in aquatic ecosystems.

Keywords: Hg stable isotopes; Hg sources; MMHg photodegradation; dissolved organic matter.

Synopsis: Hg stable isotopes helps decipher Hg sources and transformations along gradients in the Baltic Sea and highlights the importance of terrestrial DOM on the extent of MMHg photodegradation.

INTRODUCTION

Humans are predominantly exposed to mercury (Hg) through the consumption of seafood products[1], in which Hg is mostly present as the neurotoxic compound monomethylmercury (MMHg). Concentrations of MMHg in seafood depend on the efficiency of MMHg bioconcentration from water to plankton and its bioamplification through food webs.[2,3] The presence of inorganic Hg (the substrate for MMHg formation) in aquatic ecosystems can be ascribed to multiple sources: direct atmospheric deposition (dry and wet), watershed runoff and industrial discharges. It is critical to know the contribution from each source to fish MMHg in a given ecosystem to develop efficient policies of Hg emissions reduction.[4] The production of MMHg is essentially a biotic process controlled by the interplay between the activity of specific methylating microorganisms and the bioavailability of inorganic Hg.[5] On the contrary, the degradation of MMHg can proceed through several biotic and/or abiotic pathways with photodegradation considered a major sink in the photic zone.[6,7]

Over the past two decades, measurements of Hg stable isotopes has emerged as a major tool to advance our understanding of Hg cycling in the environment. Based on their mass-dependent and mass-independent isotope fractionation (Hg-MDF and -MIF, respectively), isotopes are useful for both differentiating Hg sources with contrasted isotopic signatures and informing on the extent, mechanisms and conditions of species transformations.[8] In soils and sediments, binary or ternary mixing models have been used to discriminate between Hg originating from contaminated point sources (industrial and/or mining activities with slightly negative Hg-MDF and near zero Hg-MIF)[9–11] and background Hg sources, i.e. terrestrial inputs with largely negative Hg-MDF and Hg-MIF versus the atmospheric ones.[12–14] The contribution of atmospheric inputs is however especially difficult to estimate as both their Hg-MDF and –MIF can be highly variable in background atmosphere but especially when point-source emissions are involved.[15] Lately the use of even Hg-MIF values (Δ^{200}Hg and to a lesser extent Δ^{204}Hg) has emerged to specifically discriminate gaseous Hg inputs,[12,16] as atmospheric Hg^0 exhibits slightly negative Δ^{200}Hg values whereas Hg(II) in wet and dry depositions is characterized by slight to large positive values.[16,17]

All Hg species undergo numerous reactions in surficial environments, e.g. in the atmosphere, soils, snow and water column, before being taken up by organisms at the base of food webs but only photochemical reactions specifically induce large and characteristic Hg-MIF of odd and even isotopes.[18] The Δ^{199}Hg/Δ^{201}Hg slope has turned out to be a reliable indicator for the type of reactions involved (Hg(II) photoreduction vs MMHg photodegradation),[19] the mechanisms causing MIF (magnetic isotope effect vs nuclear volume effect),[20] and the Hg bonding environment

including the nature of the Hg ligands and the Hg to ligands ratio.[21–23] Similarly, the even Hg-MIF slopes are emerging as a new indicator of photochemical reactions occurring in the upper atmosphere.[24,25]

Hg stable isotopes are also powerful tracers to examine the environmental controls of MMHg cycling, e.g. its production depth in aquatic environments or the influence of light transmission and attenuation for its photodegradation,[26–28] by analyzing high-trophic level organisms that contain predominantly MMHg. They can also be used as ecological tracers to distinguish populations and provide unique information on animal movements and their foraging habits within ecosystems.[8,29] One important assumption underlying these studies is the absence of Hg MIF in organisms after its accumulation. This is in contrast to Hg-MDF that has been shown to occur in higher organisms, due to MMHg degradation and excretion.[8] Therefore, the MMHg isotopic signature in organisms is useful to infer the transformations it has undergone, especially its photodegradation that is mainly controlled by light radiation intensity and penetration as well as the chemical speciation of aqueous MMHg.[30,31]

Direct photolysis of MMHg is not possible under environmental conditions in aquatic ecosystems and the presence of dissolved organic matter (DOM) is required to trigger MMHg photodegradation.[7] Both the concentration and composition of DOM influence the extent of photodegradation through their effect on light transmission, production/consumption of reactive oxygen species, and Hg complexation.[32,33] The rates of MMHg photodegradation increase with dissolved organic carbon (DOC) concentrations till a breaking point (5 – 10 mg L^{-1}) after which the reaction is inhibited due to either shading or the scavenging of reactive oxygen species.[27,34,35] The complexation of MMHg by thiol groups has been found to be key as it weakens the Hg-C bond[36–38] and photodegradation has been shown to be more efficient when aromatic DOM is involved.[39,40] Accordingly, differences in MMHg photodegradation rates depending on the size or chemical fraction of DOM have been evidenced[41,42] and in wetlands and rice fields, higher MMHg losses were related to optical signatures of less labile, humic DOM.[43] However, the effect of DOM quality on the extent of MMHg photodegradation has not been evaluated at large scale in aquatic ecosystems.

In this study, we investigated Hg stable isotopic signature in sediment, seston and fish samples from the various basins of the Baltic Sea, a semi-enclosed sea with a large freshwater influence and spatial gradients in several key factors known to influence Hg species transformations and bioaccumulation including salinity, redox conditions, light, ice cover, presence of algae as well as OM concentration and quality. The salinity, temperature and nutrient loads are highest in the southern Baltic Sea leading to higher photosynthetic primary production rate and thus to

the development of large oxygen depleted areas with a sustained production of MMHg in the anoxic part of the water column.[44] Because of a lower temperature and larger OM inputs by river discharge in the northern Baltic Sea, the primary production is lower and the fraction of allochthonous to autochthonous OM is higher, which can impact both MMHg production, bioavailability and bioaccumulation.[45,46] We combined concentrations and speciation data with the isotopic signatures observed in the various compartments, trophic levels and spatial origin to provide new insights into the sources, bioaccumulation and transformations of Hg species in this large brackish ecosystem. We especially discuss the factors controlling MMHg photodegradation in the various basins and highlight the impact of the terrestrial DOM gradient on the extent of this reaction.

EXPERIMENTAL SECTION

Study site, sample collection and ancillary data

Sample types and stations from which sediment, plankton and fish samples were collected are presented in Figure 1 together with our division of the sampling locations into four Baltic Sea basins. Surface sediment samples (0 – 2 cm, n = 29) were obtained from the Swedish Geological Survey archive and were selected from a variety of sites (coastal vs offshore and contaminated vs pristine) to provide a sufficient spatial coverage and representation of various sources of Hg. Samples were collected between 1992 and 2007 as part of Sweden's national environmental monitoring program that takes place every 6th year and stored freeze-dried in closed containers. Seston samples (n = 24) were collected using a 90 µm mesh-size net during field campaigns in July-August 2015 and June-November 2016 that have been previously described.[44] In short, on cruises in the Baltic Proper and Kattegat, samples were collected from the upper 20 m of the water column but the net was closed before breaching the surface to avoid getting filamentous cyanobacteria, often present at the sea surface, in the net. On cruises in the Bothnian Bay and Sea, samples were collected from the entire water depth at each sampling station (8 - 125 m). Samples were always transferred from the net to 500 ml HDPE bottles and frozen on board.

Herring and cod samples (n = 45, female specimen of 2-5 and 2 years age, respectively) were obtained from the Swedish Environmental Specimen Bank. They were collected in fall 2013 as part of the Marine Monitoring Programme for Contaminants in Marine Biota and their length, age, weight as well as their muscle $\delta^{15}N$ and $\delta^{13}C$ values were measured.[47] The latter were then corrected for lipids according to equation 1:[48]

$$\delta^{13}C_{norm} = \delta^{13}C_{untreat} - 3.32 + 0.99 \times C{:}N \qquad \text{eq 1}$$

The Baltic herring (*Clupea harengus*) is found in the various basins throughout the Baltic Sea whereas the Atlantic cod (*Gadus morhua*) is not present in the northern part due to the low salinity. Moreover, there are two distinct stocks of cod, a western and an eastern one, that partially mix in the southern part of the Baltic Sea.[49] The trophic levels (TL) of fishes were calculated with equation 2 by matching the $\delta^{15}N$ data from the fish with $\delta^{15}N$ of mussels based on areas of collection in the Baltic Sea.

$$TL_{fish} = (\delta^{15}N_{fish} - \delta^{15}N_{mussels})/TLF + 2 \qquad \text{eq 2}$$

where TLF is the trophic level fractionation of $\delta^{15}N$ and the trophic position of mussels are assumed to be two. We use a value of 2.4 ‰ for the trophic level fractionation as previously found for the Baltic Sea,[50] and $\delta^{15}N$ values for mussels from previous studies.[47,51]

Cumulated PAR and UV irradiance data were obtained from the Swedish Meteorological and Hydrological Institute (SMHI) and averaged over the period 2012 – 2013. Salinity, secchi depth and concentrations of humic substances were also obtained from SMHI and are from monthly cruises conducted across the Baltic Sea. When available, salinity and humic substances were taken from the same station as the fish and when not we used the nearest available station. Salinity and humic substances were averaged over the top 50 m depth. DOC concentrations were obtained from Seidel et al.[52]

Measurements of Hg concentrations and isotopic composition.

HgT concentrations in sediments and some fish were available through the Swedish national environmental monitoring,[47,53] but seston samples as well as some fish samples for which HgT values were not available were analyzed with total Hg analyzers (either Leco AMA254 or Milestone DMA-80). MMHg concentrations in sediments, seston and fish were determined after acidic or basic extraction of freeze-dried samples using species-specific isotope dilution and (thermal desorption) gas chromatography inductively coupled plasma mass spectrometry according to established protocols.[54,55] Extraction and/or quantification of Hg total and species concentrations were validated with various certified reference materials, i.e. IAEA 405, CNRC TORT-2&3, JCR ERM CE-464 and BCR-414, and NIST SRM-1947.

For stable isotopes analysis, sediments and seston samples (0.5 g) were first extracted with a 3:1 HNO_3/HCl mixture for 12 h at 85 °C, then H_2O_2 was added and samples were further heated at 85 °C for 12 h. Fish samples (0.2 g) were extracted for 12 h at 85 °C with a 2:1 HNO_3/ H_2O_2 mixture. Analyses were carried out with a multicollector-inductively coupled plasma-mass spectrometer (MC-ICP-MS, Nu Instruments) using either introduction with cold vapor generation (CVG) or dual amalgamation on gold (DA-Au) using a Tekran 2600 system for low-concentrated samples.[56] In both cases, a desolvation nebulization system (DSN-100, Nu Instrument) was used to introduce a certified thallium solution (NIST-SRM-997) for instrumental mass-bias correction using the exponential fractionation law. We used a standard-sample bracketing system to calculate δ values (in ‰) relative to the reference Hg standard NIST SRM 3133. Reference materials NIST-8610 (UM-Almaden), -1944 and -1947, ERM BCR 414 and

CE-464 were used as secondary standards (Table SI-1). Isotopic ratios were calculated by the Linear Regression Slope (LRS) method for the DA-Au introduction technique as described previously.[56] The common δ notation is used to express the Hg isotopic compositions:

$$\delta^{xxx}Hg\ (‰) = \left[\frac{\frac{^{xxx}Hg}{^{198}Hg}_{sample}}{\frac{^{xxx}Hg}{^{198}Hg}_{NIST\,3133}} - 1\right] \times 1000$$

where xxx can be either 204, 202, 201, 200 or 199 and $(^{xxx}Hg/^{198}Hg)_{NIST\ 3133}$ is the averaged isotopic ratio of the two bracketing standards. The Δ notation is used to express the mass independent fractionation (MIF), calculated as $\Delta^{xxx}Hg = \delta^{xxx}Hg - \beta_{kin} \times \delta^{202}Hg$ where $\beta_{kin} = \ln(m_{198}/m_{xxx})/\ln(m_{198}/m_{202})$.[57]

RESULTS AND DISCUSSION

Sedimentary Hg reflects the mixing between terrestrial, industrial and atmospheric sources. As sediment samples were selected to represent both coastal and offshore as well as contaminated and pristine environments, the range of HgT concentrations is large, from 64 to 10 690 ng g^{-1} with a median value of 140 ng g^{-1} (interquartile range (IQR) = 167) (Table SI-2). MMHg concentrations range from 0.1 to 13.6 ng g^{-1} and contribute on average 0.7 ± 0.7 % to HgT, similar to other coastal environments and great lakes.[58,59] Our HgT values are overall in agreement with two recent studies that demonstrated a strong anthropogenic pollution during the second half of the past century that overall increased Hg concentrations in the Baltic Sea sediments over its pre-industrial background (20 – 50 ng g^{-1})[60] and also led to high Hg concentrations in some local hotspots (industrial and war waste sites).[60,61] δ^{202}Hg in sediments ranges from - 2.3 to - 0.1 ‰ (Table SI-2) and with the exception of 4 outliers, it is linearly and negatively correlated to 1/HgT (Figure SI-1, r^2 = 0.5, p-value = 10^{-4}). This trend indicates mixing between a lighter Hg end-member with an average δ^{202}Hg value of - 2.18 ± 0.45 ‰ (calculated for an average background HgT concentration of 35 ng g^{-1}) and a heavier Hg end-member with an average δ^{202}Hg value of - 0.55 ± 0.11 ‰ (y-intercept in Figure SI-1), the latter being very similar to the value previously found by Gehrke.[62] Although the data are relatively scattered, no specific trend is apparent between basins suggesting that both end-members are relatively homogeneous across the sites investigated. The heavy end-member value is typical of industrial sources and matches the δ^{202}Hg value reported for cinnabar (HgS)[63] as well as the values previously found in sediments from polluted sites across Sweden.[10] With respect to their concentrations, the 4 outliers exhibit a much lighter isotopic composition with δ^{202}Hg values of about - 2.3 ‰ and slightly positive odd-MIF values (Δ^{199}Hg from 0.05 to 0.10 ‰). Their isotopic composition is very similar to those reported for a coastal site polluted by elemental Hg (exhibiting specifically low δ^{202}Hg values) located in the Bothnian Sea south of these 4 samples.[10] The light end-member is close to the negative δ^{202}Hg values previously reported for boreal forest soils (- 2.6 to - 2.9 ‰), which results from the large MDF that occur during uptake and oxidation of atmospheric gaseous Hg by foliage.[64,65] This MDF is conserved when Hg is transferred to soils and adjacent aquatic ecosystems[66] and the higher δ^{202}Hg values in sediments compared to soils can reflect both the photoreduction of this terrestrially derived Hg(II) in the water column[67] and its mixing with heavier Hg inputs, i.e. atmospheric and/or industrial Hg brought in the various basins by direct deposition, river discharges,[45] and/or sediment redistribution.

The range of Hg odd-MIF values in sediments is narrow (Table SI-1, Δ^{199}Hg = -0.16 - 0.10 ‰) as commonly observed,[18] There is a positive trend between Δ^{199}Hg and 1/HgT in sediments but it is not significant (Figure SI-1, p-value = 0.35). However, sediments with low Hg content exhibit significantly higher Δ^{199}Hg than values previously observed in boreal forest soils (- 0.5 to - 0.25 ‰), suggesting again mixing with atmospheric Hg (wet and dry) and/or photoreduction of Hg(II) before its deposition to sediments. The Δ^{199}Hg/Δ^{201}Hg slope in sediments is indeed 1.1 ± 0.3 (not shown, r^2 = 0.59, p-value = 3.10^{-4}) close to the one imprinted by Hg(II) photoreduction that can occur in the water column,[19,67] but also in the atmosphere.[25] Regarding Hg even-MIF, Δ^{200}Hg values ranged from -0.04 to 0.08 ‰ and Δ^{204}Hg from -0.22 to 0.14 ‰ (Table SI-2, Figure 3), which is also similar to previous observations in freshwater and coastal sediments.[12,68,69] No significant relationships were found between Hg even-MIF and concentrations and the data scattering render their interpretations difficult. The discrimination of Hg sources to sediments is difficult as their Hg isotopic signature results from the mixture of multiple sources and processes inducing isotopic fractionation. Isotopic signatures of soils and especially atmospheric Hg, for which both Hg-MDF and –MIF values can be highly variable, need to be characterized at a regional level before the contribution of each source of Hg to the Baltic Sea sediments can be better deciphered.

Biota Hg concentrations and MDF are primarily controlled by trophic level. HgT in seston range from 1.5 to 60 ng g^{-1} (d.w., average 18 ± 16 ng g^{-1}, n = 23) with the highest values found at the northernmost, least saline station Harufjarden (31 ± 16 ng g^{-1}, Figure SI-2). The percentage of MMHg in seston vary over the full range, from 0.5 to 98 % and averages 27 ± 22 % of HgT. In fish muscle, HgT concentrations range from 34 to 530 ng g^{-1} (d.w.) and average 137 ± 102 ng g^{-1} to which MMHg contribution is constant at 93 ± 3 %. The lowest concentrations are found in herrings from the Bothnian Sea offshore station (48 ± 12 ng g^{-1}, Table SI-3) while the highest are found in cod from the Fladen station (312 ± 135 ng g^{-1}) which is explained by the higher trophic level of cod compared to herring. Overall, the trophic magnification slope determined from our samples is 0.14 ± 0.08 (Figure SI-3a, r^2 = 0.78), which is similar to the value previously reported for a pelagic food chain from the Baltic Sea,[70] and also in line with values compiled by Lavoie et al.[2] for a variety of ecosystems (average slope for HgT = 0.16 ± 0.11).

With the exception of one outlier (δ^{202}Hg = -2.47 ‰), the δ^{202}Hg values in seston range from -1.75 to -0.26 ‰ and averaged -1.1 ± 0.5 ‰ (1 SD, Figure 2a and Table SI-4). These are very similar to sediments in range and average

value (-1.2 ± 0.6 ‰ , 1 SD), which stems from the seston samples being dominated by Hg(II). There is only a weak relationship between δ^{202}Hg in seston and 1/HgT (Figure SI-4a), reflecting both the presence of MMHg in different proportions and the fact that seston and sediments do not accumulate Hg(II) with the exact same signature (see below). As expected, the δ^{202}Hg values in fish are higher (- 0.29 to 0.73 ‰, Figure 2b) and the range between the lowest and highest value is smaller (1.0 ‰) than for seston (1.5 ‰) and sediments (2.2 ‰). This reflects a homogenization (decrease in variability) of the Hg isotopic composition higher up in the food webs with higher organisms displaying a more integrative MMHg isotopic signature. The average δ^{202}Hg from our fish samples is 0.27 ± 0.23 ‰ (1 SD) with the lowest values found in herring from Angskarsklubb (-0.08 ± 0.15 ‰, 1 SD) whereas the highest values are found in herring from Fladen and Bothnian Sea offshore (0.55 ± 0.12 and 0.51 ± 0.09 ‰, respectively, 1 SD). Overall, δ^{202}Hg values in biota increase on average by 0.5 ± 0.1 ‰ per trophic level (Figure SI-3b), consistent with values found in the Chinese Bohai Sea.[69] Higher trophic level biota thus accumulates a higher share of heavier Hg isotopes in MMHg (Figure SI-3c) and variations in δ^{202}Hg among biota are mostly explained by their trophic level. However, many seston samples from the Bothnian Bay and cod from Fladen are below this trend revealing the accumulation of isotopically lighter Hg species. For seston from the Bothnian Bay, we prescribe this to the terrestrial inputs, most important to this basin, carrying lighter Hg isotopes. For cod from Fladen, they have been shown to have a more pronounced benthic feeding strategy as they live in shallow waters,[71] and they are therefore likely to accumulate more MMHg originating from sediments, that is less (photo)fractionated, compared to the pelagic herring and cod from SO Gotland that live in deeper waters.

Odd Hg-MIF in seston reflects in situ photochemical reactions and even Hg-MIF atmospheric Hg sources. Δ^{199}Hg values in seston range from -0.04 to 2.18 ‰ (Table SI-4) and seston samples are found in intermediate positions, depending on their trophic level and Hg speciation, between the background sediment and the fish signatures on the Δ^{199}Hg - δ^{202}Hg plot (Figure 2a). Overall, the Δ^{199}Hg/Δ^{201}Hg slope in seston is 0.92 ± 0.11 (Figure 2c), close to the slope produced by the photoreduction of Hg(II).[19] This results from the predominance of Hg(II) over MMHg (73 vs 27 % average, respectively) and indicates that most of the Hg present in seston has undergone some photochemical processing, either Hg(II) photoreduction or MMHg photodegradation. However, the Δ^{199}Hg signal in seston is also positively albeit weakly correlated to the % MMHg (Figure SI-4b, R^2 = 0.50) and negatively to the %

Hg(II) (not shown), suggesting that the MIF signal is dominated by the contribution of MMHg in seston of higher trophic level. The weak correlation between MIF values and % MMHg is likely due to the spatial and seasonal variability of photochemical processes affecting both MMHg and Hg(II) in the water column before their uptake. Photochemical reactions are affected by a number of parameters, among which light radiation intensity and wavelength as well as DOM concentrations are the most important,[30,32,72] and all of them vary both spatially and temporally across the Baltic Sea (see below).

Even Hg-MIF values in sediment, seston and fish are presented in Figure 3. Median Δ^{200}Hg values in seston and fish are higher than in sediments (0.12, 0.03 and 0.01 ‰, respectively), which is consistent with previous studies on aquatic invertebrates and fish,[26,27,73–75] but it is particularly noteworthy that several values are above 0.2 ‰ in seston. Hg isotopic data in phyto- or zooplankton are particularly scarce,[75,76] but the maximum value of 0.58 ‰ observed in our study is to the best of our knowledge the highest reported in such samples. These values are actually similar to values reported for seawater in the Canadian Arctic[77,78] and higher than many values reported for precipitations collected at low latitudes in the temperate zone,[65,79–83] with the exception of samples collected in Peterborough (44 °N) where Δ^{200}Hg reached up 1.2 ‰ in both rain and snow.[17] The median Δ^{200}Hg value is higher for seston than fish but this could result from a sampling bias as there are fewer seston samples that were not collected in the same year and their distribution is skewed towards northern stations compared to fish. In seston, the Δ^{200}Hg values are higher than the Δ^{204}Hg ones and even though not significant, the Δ^{200}Hg/Δ^{204}Hg slope (-0.28, $r^2 = 0.12$, p-value > 0.05, Figure SI-4c) is very similar to the slopes reported for precipitations and marine biota.[15,16] Our data therefore strengthen previous studies in suggesting that pelagic plankton and invertebrates preferentially accumulate Hg(II) originating from wet depositions that are characterized by positive Δ^{200}Hg and negative Δ^{204}Hg values,[65,80,84] or MMHg formed from this Hg(II) pool.

It has been proposed that even Hg-MIF values in precipitation increases with latitude, implying an upper atmosphere origin of even-MIF.[82,85] Our data support this (i) as the Baltic Sea is located north of Peterborough (roughly from 55 to 65 °N) and (ii) because there is an apparent gradient in Δ^{200}Hg average values along the Baltic Sea, from 0.06 ± 0.20 ‰ in the south, western basin (Kattegat) to 0.22 ± 0.20 ‰ in the northern basin (Bothnian Bay). The highest even-MIF values are found in the northern basin which can be explained by the fact that (i) deep stratospheric intrusions are likely more common towards the north as the troposphere height decreases towards

the poles,[85] and (ii) snow precipitation is more important in this basin (> 40 % of total precipitations vs 20 % in the south)[86] and the highest even-MIF values have been reported in snow until now.[17] Similarly to odd-MIF, the Δ^{200}Hg signal in seston is also overall positively (albeit weakly) correlated to the % MMHg (Figure SI-4d, $R^2 = 0.37$, p-value < 0.005), which indicates that at higher tropic levels in the food web the even-MIF signal is eventually dominated by the contribution of MMHg to total Hg. However, some elevated values are also found in samples with MMHg < 30 %, demonstrating an important contribution of Hg(II) in some cases. Our data suggests that the analysis of seston is promising to discriminate the contribution of Hg wet deposition to the water column. It seems to be able to reflect this atmospheric signature at a higher temporal and spatial resolution compared to fish that accumulates a broader temporal and spatial average MMHg signal or sediments, where it is largely diluted by the terrestrial and anthropogenic Hg inputs.

Odd Hg-MIF in fish reveals basin-specific MMHg photodegradation patterns. Odd Hg-MIF is found in all fish samples, whatever the fish species or sub-basins, with Δ^{199}Hg ranging from 0.33 to 3.04 ‰ and Δ^{201}Hg from 0.21 to 2.26 ‰ (Figure 2 and Table SI-3). The Δ^{199}Hg/Δ^{201}Hg slope is 1.31 ± 0.02 (Figure 2c, linear fit, no weighting, p-value < 0.005, n = 51) when considering all fish samples, which is typical for freshwater fish as it reflects the slope imprinted during MMHg photodegradation in freshwater with excess DOM compared to MMHg.[18,19,23,27,73,76,87] However, cod from Fladen present a lower Δ^{199}Hg/Δ^{201}Hg ratio of 1.08 ± 0.22 (n = 5) compared to the other fish even if their MMHg content is similar (90.9 – 98.6 %). This likely results from both their more pronounced benthic feeding that lead to the accumulation of both pelagic and benthic MMHg that is less or not photodegraded, and their migration strategy. It has been evidenced that most individuals from the population in Kattegat (Fladen) undertake spawning migrations towards the North Sea,[88] and it is well established that a lower slope is imprinted during MMHg photodegradation in low DOM marine waters.[18,28,29,69,89]

There is a good separation of the various fish populations in the δ^{202}Hg - Δ^{199}Hg space (Figure 2b), suggesting that they could be discriminated based on their Hg isotopic signatures as previously demonstrated for juvenile Seabass at the European scale.[29] This separation stems partly from the multiple Hg sources entering the food web and the food web structure as discussed above but also from a different degree of MMHg photodegradation between basins controlled by a combination of environmental factors. There is a clear upward shift from an average Δ^{199}Hg of 0.53

297 ± 0.29 ‰ in herrings from Ostergarnsholm (Baltic Proper) to 2.58 ± 0.48 ‰ in Harufjarden (Bothnian Bay). Contrary
298 to seston, Δ^{200}Hg values in herring are similar in the northern and central stations (from 0.03 ± 0.05 ‰ for the Baltic
299 Proper offshore to 0.08 ± 0.06 ‰ for Holmoarna, vs -0.01 ± 0.04 ‰ for Fladen, Figure 4a). This result demonstrates
300 that MMHg is formed from an homogenous pool of Hg with respect to atmospheric sources and therefore that the
301 odd Hg-MIF trends observed are due to differences in MMHg photodegradation rates.
302 The maximum Δ^{199}Hg values found in the Baltic Sea are relatively low compared to values observed in pelagic fish
303 from other fresh or marine waters (e.g. Lake Baikal, high altitudes Tibetan lakes, North American great Lakes or
304 the Pacific ocean)[76,90,73,28] that often reach 6 – 7 ‰, sometimes up to 9 ‰, indicating that the extent of MMHg
305 photodegradation in the Baltic Sea is relatively limited. Based on a MIF enrichment factor of 14.3 ‰,[22,23] we
306 calculated that the extent of MMHg photodegradation before incorporation into the food web averages 4 - 5 % in
307 the central Baltic Sea (Baltic Proper), 6 % in the Kattegat and up to 16 % in the northern, less saline basins (Bothnian
308 Sea and Bay). This limited MMHg photodegradation can be explained by a combination of factors, i.e. the amount
309 of incident light, its penetration in the water column and the residence time of MMHg in the photic zone. Solar
310 radiation is about 2-5 times lower in boreal regions compared to temperate or tropical ones and the light penetration
311 in ice-free water of the Baltic Sea is comparably low. The secchi depth averages 11 m in the south Kattegat strait
312 to 3 - 5 m in the Bothnian Bay (Figure SI-5a) compared to e.g. about 15 m in the Laurentian Great Lakes[73] and 45
313 m in the Atlantic and Pacific oceans.[28] The light penetration and residence time of Hg (about one year)[45] are limited
314 by relatively high concentrations of DOM and/or POM throughout the entire Baltic Sea compared to marine waters
315 and recurrent “massive” algae blooms that occur especially in the central part of the Baltic Sea, starting with diatoms
316 and dinoflagellates in spring which are then replaced by filamentous cyanobacteria over the summer.[91] It is
317 noteworthy that the lowest Δ^{199}Hg values are indeed observed at the Ostergarnsholm and Baltic proper offshore
318 stations where algae blooms form a thick cover that severely decreases light penetration in the water column but
319 also likely protects Hg species from light exposure following their internalization. Moreover, light penetration is also
320 limited by ice cover in the Baltic Sea and this certainly lower the extent of MMHg photodegradation overall,
321 especially in the northern basins (Bothnian Sea and Bay), as already demonstrated in other northern ecosystems.[92]
322 The Δ^{199}Hg values in fish presented here are thus likely lower than expected as the maximum ice extents were
323 above average from 2011 to 2013 (177 000 to 309 000 km^2 compared to an average value of 140 000 km^2 over the

past 30 years). On the contrary, values in seston might be higher than expected as ice extents over 2015 – 2016 were lower than average (51 000 to 110 000 km^2).[93] Finally, production of MMHg in the anoxic parts of the water column has been previously established in the Baltic Proper basin[44] and deep waters could thus also contribute a non or less fractionated MMHg to biota. Further studies are required to clarify this point as it was previously found that turbulent diffusion across the hypoxic-anoxic interface was a likely source of MMHg to the hypoxic zone but not to normoxic waters where fish spend most of their time.[44]

MMHg photodegradation is driven by the terrestrial fraction of DOM. There is a negative relationship between Δ^{199}Hg in herring and incident light irradiance over the inner Baltic Sea (Kattegat excluded), both with respect to UV (Figure 4a) and PAR (Figure SI-5a). This trend cannot be explained by light penetration as the secchi depth overall decreases from south to north and therefore shows no correlation with Δ^{199}Hg (Figure SI-5b&c).[94] The Δ^{199}Hg value in Kattegat is higher than expected from the trend and this is likely the result of the larger irradiance and deeper light penetration in this basin, about twice that of the others. The negative relationship between Δ^{199}Hg and light penetration in the inner Baltic Sea (Baltic Proper, Bothnian Sea and Bothnian Bay) is a surprising finding as previous studies have found a positive correlation between the extent of MMHg photodegradation and light penetration in both fresh and marine waters.[27,28,73] There is also a clear negative correlation of Δ^{199}Hg values with salinity over the inner Baltic Sea (Figure SI-6a, $y = -0.5 + 3.7$, $r^2 = 0.9$, Kattegat excluded) that demonstrates the importance of freshwater inputs to enhance photodegradation of MMHg along the mixing zone. This increase in Δ^{199}Hg towards the northern, less saline waters, is well explained by the concentration of humic substances (Figure SI-7a, slope = 0.18, $r^2 = 0.8$), that also increases from an average of 8.3 ± 0.2 µg L^{-1} in Ostergarnsholm to 17.5 ± 1.5 µg L^{-1} in Harufjarden (while DOC concentrations only increases from 3.5 to 3.9 mg L^{-1}, Figure SI-7b).

The contribution of terrestrial DOC to the total DOC in the Baltic Sea has previously been estimated to increase from about 40 % in the Baltic Proper to 50 % in the Bothnian Sea and up to 80 % in the Bothnian Bay.[95] In this study from Deutsch et al.,[95] δ^{13}C values in high molecular weight DOM (> 1 kDa) ranged from about -27 to -25 ‰ across the Baltic Proper, Bothnian Sea and Bay basins and were found to be linearly correlated with salinity values ranging from 2 to 7 psu. Here we find that across the inner Baltic basins, Δ^{199}Hg values in herring are negatively correlated to the δ^{13}C values measured in the fish themselves, ranging from about – 26 to -20 ‰ (Figure 4b, y = -

0.38 - 7.36, r^2 = 0.81, p-value < 0.001, regression performed on individual points). The $\delta^{13}C$ values also point to two "sub-populations" of herring in the northern Bothnian Bay (Harufjarden station) with distinct $\Delta^{199}Hg$ values (average 1.9 ± 0.1 and 2.9 ± 0.1 ‰, Figure 4b). This suggests that the gradient in humic substances concentrations from coastal to open-sea conditions generally observed in the Baltic Sea has a strong impact on the extent of MMHg photodegradation. Particularly high humic substances concentrations up to 70 µg L^{-1} are observed along the Bothnian Bay coast (Figure SI-6b). Altogether, the relationships between Hg odd-MIF and salinity, concentrations of humic substances and $\delta^{13}C$ strongly point to the terrestrial fraction of DOC as the key factor controlling the photodegradation of MMHg along the salinity gradient of this large estuarine ecosystem.

To the best of our knowledge, this is the first study to demonstrate at the ecosystem scale that MMHg photodegradation is enhanced by increasing low concentrations of terrestrial DOM. The importance of low molecular weight, aromatic DOM for the MMHg photodegradation reaction was previously demonstrated in several lab or field experiments with addition of model compounds or purified DOM extracts. For example, additions of fulvic acid up to several ten's of mg L^{-1} in natural waters were found to promote the reaction.[38,39,41] On the other hand, the negative effect of high molecular weight humic acid has been demonstrated with purified extracts,[41] but also by field studies focused on lakes with high DOC levels.[27,35] These latter studies have overall evidenced a decrease of the photodegradation extents with increasing DOC concentrations but the tipping point between enhancement and inhibition remains overall poorly defined. However, it has been suggested that 6 - 7 mg L^{-1} of DOC seem to be optimal conditions for MMHg photodegradation in natural waters,[23,34] and here we found it to be at its highest where the more terrestrial and highest concentrations of DOC are found in the Baltic Sea (i.e. averages of 16 – 18 µg L^{-1} for humic substances and 3.9 mg L^{-1} for DOC at Holmoarna and Harufjarden). It gives a new perspective to the negative relationship previously observed between MMHg and humic OM in the northern Baltic Sea, which was hypothesized to be caused by a reduced availability of Hg(II) for microbial MMHg formation.[46] Our findings now strongly suggests that MMHg photodegradation also plays an important role for this negative relationship. It remains to be tested if terrestrial OM driven photodegradation is an important MMHg sink also in other types of coastal seas with higher light irradiance and penetration (e.g. in temperate regions). Based on our results it can be expected that the magnitude of this MMHg sink will increase with the large increased delivery of terrestrial OM to lakes, rivers and coastal ecosystems expected especially in the world's northern regions with climate and other global changes. Further studies are thus required to quantitatively assess the impacts of the

various OM fractions on MMHg photodegradation, especially the opposing effects of low and high molecular weight compounds, in order to better predict future MMHg concentrations in water and biota.

Supporting Information.

Hg isotopic composition of the various reference materials; Hg concentrations and isotopic composition in sediments from the Baltic Sea; δ^{202}Hg versus 1/HgT and Δ^{199}Hg versus δ^{202}Hg in sediments from the various basins of the Baltic Sea; Hg concentrations and isotopic composition in fish from the Baltic Sea; Hg concentrations and isotopic composition in seston from the Baltic Sea; HgT concentration in seston and fishes versus latitude and salinity; log10HgT concentrations versus δ15N, δ^{202}Hg versus trophic level and % MMHg versus trophic level for all biota samples (seston and fishes); δ^{202}Hg versus 1/HgT; Δ^{199}Hg versus % MMHg; Δ^{200}Hg versus Δ^{204}Hg and Δ^{200}Hg versus % MMHg in seston samples from the Baltic Sea; Δ^{199}Hg in herring from the various basins versus incident PAR irradiance, Secchi depth in the various basins versus incident PAR irradiance and Δ^{199}Hg in herring from the various basins versus Secchi depth.; Δ^{199}Hg in herring from the various basins as a function of concentrations of humic substances and DOC.

Acknowledgments.

This work was funded by the Swedish research council FORMAS (grants 2014-1088 and 2021-00942). We warmly acknowledge Aleksandra Skrobonja for the Hg total and speciation analyses of the seston samples. We thank the Swedish Environmental Specimen Bank, part of the Swedish Museum of Natural History, for providing fish samples and the Swedish Geological Survey for providing sediment samples for the study.

REFERENCES

(1) Sheehan, M. C.; Burke, T. A.; Navas-Acien, A.; Breysse, P. N.; McGready, J.; Fox, M. A. Global Methylmercury Exposure from Seafood Consumption and Risk of Developmental Neurotoxicity: A Systematic Review. *Bulletin of the World Health Organization* **2014**, *92* (4), 254-269F. https://doi.org/10.2471/BLT.12.116152.

(2) Lavoie, R. A.; Jardine, T. D.; Chumchal, M. M.; Kidd, K. A.; Campbell, L. M. Biomagnification of Mercury in Aquatic Food Webs: A Worldwide Meta-Analysis. *Environ. Sci. Technol.* **2013**, *47* (23), 13385–13394. https://doi.org/10.1021/es403103t.
(3) Wu, P.; Kainz, M. J.; Bravo, A. G.; Åkerblom, S.; Sonesten, L.; Bishop, K. The Importance of Bioconcentration into the Pelagic Food Web Base for Methylmercury Biomagnification: A Meta-Analysis. *Science of The Total Environment* **2019**, *646*, 357–367. https://doi.org/10.1016/j.scitotenv.2018.07.328.
(4) Blanchfield, P. J.; Rudd, J. W. M.; Hrenchuk, L. E.; Amyot, M.; Babiarz, C. L.; Beaty, K. G.; Bodaly, R. A. D.; Branfireun, B. A.; Gilmour, C. C.; Graydon, J. A.; Hall, B. D.; Harris, R. C.; Heyes, A.; Hintelmann, H.; Hurley, J. P.; Kelly, C. A.; Krabbenhoft, D. P.; Lindberg, S. E.; Mason, R. P.; Paterson, M. J.; Podemski, C. L.; Sandilands, K. A.; Southworth, G. R.; St Louis, V. L.; Tate, L. S.; Tate, M. T. Experimental Evidence for Recovery of Mercury-Contaminated Fish Populations. *Nature* **2021**, 1–5. https://doi.org/10.1038/s41586-021-04222-7.
(5) Regnell, O.; Watras, Carl. J. Microbial Mercury Methylation in Aquatic Environments: A Critical Review of Published Field and Laboratory Studies. *Environmental Science & Technology* **2019**, *53* (1), 4–19. https://doi.org/10.1021/acs.est.8b02709.
(6) Barkay, T.; Gu, B. Demethylation–The Other Side of the Mercury Methylation Coin: A Critical Review. *ACS Environ. Au* **2021**. https://doi.org/10.1021/acsenvironau.1c00022.
(7) Luo, H.; Cheng, Q.; Pan, X. Photochemical Behaviors of Mercury (Hg) Species in Aquatic Systems: A Systematic Review on Reaction Process, Mechanism, and Influencing Factor. *Science of The Total Environment* **2020**, *720*, 137540. https://doi.org/10.1016/j.scitotenv.2020.137540.
(8) Tsui, M. T.-K.; Blum, J. D.; Kwon, S. Y. Review of Stable Mercury Isotopes in Ecology and Biogeochemistry. *Science of The Total Environment* **2019**, 135386. https://doi.org/10.1016/j.scitotenv.2019.135386.
(9) Foucher, D.; Ogrinc; Hintelmann, H. Tracing Mercury Contamination from the Idrija Mining Region (Slovenia) to the Gulf of Trieste Using Hg Isotope Ratio Measurements. *Environ. Sci. Technol.* **2009**, *43* (1), 33–39.
(10) Wiederhold, J. G.; Skyllberg, U.; Drott, A.; Jiskra, M.; Jonsson, S.; Björn, E.; Bourdon, B.; Kretzschmar, R. Mercury Isotope Signatures in Contaminated Sediments as Tracer for Local Industrial Pollution Sources. *Environmental Science & Technology* **2014**, 141201133154006. https://doi.org/10.1021/es5044358.
(11) Gray, J. E.; Pribil, M. J.; Higueras, P. L. Mercury Isotope Fractionation during Ore Retorting in the Almadén Mining District, Spain. *Chemical Geology* **2013**, *357*, 150–157. https://doi.org/10.1016/j.chemgeo.2013.08.036.
(12) Lepak, R. F.; Yin, R.; Krabbenhoft, D. P.; Ogorek, J. M.; DeWild, J. F.; Holsen, T. M.; Hurley, J. P. Use of Stable Isotope Signatures to Determine Mercury Sources in the Great Lakes. *Environ. Sci. Technol. Lett.* **2015**, *2* (12), 335–341. https://doi.org/10.1021/acs.estlett.5b00277.
(13) Meng, M.; Sun, R.; Liu, H.; Yu, B.; Yin, Y.; Hu, L.; Shi, J.; Jiang, G. An Integrated Model for Input and Migration of Mercury in Chinese Coastal Sediments. *Environ. Sci. Technol.* **2019**, *53* (5), 2460–2471. https://doi.org/10.1021/acs.est.8b06329.
(14) Jung, S.; Kwon, S. Y.; Li, M.-L.; Yin, R.; Park, J. Elucidating Sources of Mercury in the West Coast of Korea and the Chinese Marginal Seas Using Mercury Stable Isotopes. *Science of The Total Environment* **2022**, *814*, 152598. https://doi.org/10.1016/j.scitotenv.2021.152598.
(15) Kwon, S. Y.; Blum, J. D.; Yin, R.; Tsui, M. T.-K.; Yang, Y. H.; Choi, J. W. Mercury Stable Isotopes for Monitoring the Effectiveness of the Minamata Convention on Mercury. *Earth-Science Reviews* **2020**, *203*, 103111. https://doi.org/10.1016/j.earscirev.2020.103111.
(16) Jiskra, M.; Heimbürger-Boavida, L.-E.; Desgranges, M.-M.; Petrova, M. V.; Dufour, A.; Ferreira-Araujo, B.; Masbou, J.; Chmeleff, J.; Thyssen, M.; Point, D.; Sonke, J. E. Mercury Stable Isotopes Constrain Atmospheric Sources to the Ocean. *Nature* **2021**, *597* (7878), 678–682. https://doi.org/10.1038/s41586-021-03859-8.

(17) Chen, J.; Hintelmann, H.; Feng, X.; Dimock, B. Unusual Fractionation of Both Odd and Even Mercury Isotopes in Precipitation from Peterborough, ON, Canada. *Geochimica et Cosmochimica Acta* **2012**, *90*, 33–46. https://doi.org/10.1016/j.gca.2012.05.005.
(18) Blum, J. D.; Sherman, L. S.; Johnson, M. W. Mercury Isotopes in Earth and Environmental Sciences. *Annu. Rev. Earth. Planet. Sci.* **2014**, *42* (1), 249–269. https://doi.org/10.1146/annurev-earth-050212-124107.
(19) Bergquist, B. A.; Blum, J. D. Mass-Dependent and -Independent Fractionation of Hg Isotopes by Photoreduction in Aquatic Systems. *Science* **2007**, *318* (5849), 417–420. https://doi.org/10.1126/science.1148050.
(20) Zheng, W.; Hintelmann, H. Mercury Isotope Fractionation during Photoreduction in Natural Water Is Controlled by Its Hg/DOC Ratio. *Geochim. Cosmochim. Acta* **2009**, *73* (22), 6704–6715. https://doi.org/10.1016/j.gca.2009.08.016.
(21) Zheng, W.; Hintelmann, H. Isotope Fractionation of Mercury during Its Photochemical Reduction by Low-Molecular-Weight Organic Compounds. *J. Phys. Chem. A* **2010**, *114* (12), 4246–4253. https://doi.org/10.1021/jp9111348.
(22) Chandan, P.; Ghosh, S.; Bergquist, B. A. Mercury Isotope Fractionation during Aqueous Photo-Reduction of Monomethylmercury in the Presence of Dissolved Organic Matter. *Environ. Sci. Technol.* **2014**, 141117013917004. https://doi.org/10.1021/es5034553.
(23) Bouchet, S.; Tessier, E.; Masbou, J.; Point, D.; Lazzaro, X.; Monperrus, M.; Guédron, S.; Acha, D.; Amouroux, D. In Situ Photochemical Transformation of Hg Species and Associated Isotopic Fractionation in the Water Column of High-Altitude Lakes from the Bolivian Altiplano. *Environ. Sci. Technol.* **2022**, *56* (4), 2258–2268. https://doi.org/10.1021/acs.est.1c04704.
(24) Sun, G.; Sommar, J.; Feng, X.; Lin, C.-J.; Ge, M.; Wang, W.; Yin, R.; Fu, X.; Shang, L. Mass-Dependent and -Independent Fractionation of Mercury Isotope during Gas-Phase Oxidation of Elemental Mercury Vapor by Atomic Cl and Br. *Environ. Sci. Technol.* **2016**, *50* (17), 9232–9241. https://doi.org/10.1021/acs.est.6b01668.
(25) Fu, X.; Jiskra, M.; Yang, X.; Marusczak, N.; Enrico, M.; Chmeleff, J.; Heimbürger-Boavida, L.-E.; Gheusi, F.; Sonke, J. E. Mass-Independent Fractionation of Even and Odd Mercury Isotopes during Atmospheric Mercury Redox Reactions. *Environ. Sci. Technol.* **2021**, *55* (14), 10164–10174. https://doi.org/10.1021/acs.est.1c02568.
(26) Blum, J. D.; Popp, B. N.; Drazen, J. C.; Anela Choy, C.; Johnson, M. W. Methylmercury Production below the Mixed Layer in the North Pacific Ocean. *Nat. Geosci.* **2013**, *6* (10), 879–884. https://doi.org/10.1038/ngeo1918.
(27) Sherman, L. S.; Blum, J. D. Mercury Stable Isotopes in Sediments and Largemouth Bass from Florida Lakes, USA. *Science of The Total Environment* **2013**, *448*, 163–175. https://doi.org/10.1016/j.scitotenv.2012.09.038.
(28) Motta, L. C.; Blum, J. D.; Popp, B. N.; Drazen, J. C.; Close, H. G. Mercury Stable Isotopes in Flying Fish as a Monitor of Photochemical Degradation of Methylmercury in the Atlantic and Pacific Oceans. *Marine Chemistry* **2020**, *223*, 103790. https://doi.org/10.1016/j.marchem.2020.103790.
(29) Cransveld, A.; Amouroux, D.; Tessier, E.; Koutrakis, E.; Ozturk, A. A.; Bettoso, N.; Mieiro, C. L.; Bérail, S.; Barre, J. P. G.; Sturaro, N.; Schnitzler, J.; Das, K. Mercury Stable Isotopes Discriminate Different Populations of European Seabass and Trace Potential Hg Sources around Europe. *Environ. Sci. Technol.* **2017**, *51* (21), 12219–12228. https://doi.org/10.1021/acs.est.7b01307.
(30) Lehnherr, I.; St. Louis, V. L. Importance of Ultraviolet Radiation in the Photodemethylation of Methylmercury in Freshwater Ecosystems. *Environ. Sci. Technol.* **2009**, *43* (15), 5692–5698. https://doi.org/10.1021/es9002923.
(31) Hammerschmidt, C. R.; Fitzgerald, W. F. Iron-Mediated Photochemical Decomposition of Methylmercury in an Arctic Alaskan Lake. *Environmental Science & Technology* **2010**, *44* (16), 6138–6143. https://doi.org/10.1021/es1006934.

(32) Klapstein, S. J.; O'Driscoll, N. J. Methylmercury Biogeochemistry in Freshwater Ecosystems: A Review Focusing on DOM and Photodemethylation. *Bull. Environ. Contam. Toxicol.* **2018**, *100* (1), 14–25. https://doi.org/10.1007/s00128-017-2236-x.
(33) Yang, J.; Kim, J.; Soerensen, A. L.; Lee, W.; Han, S. The Role of Fluorescent Dissolved Organic Matter on Mercury Photoreduction Rates: A Case Study of Three Temperate Lakes. *Geochimica et Cosmochimica Acta* **2020**. https://doi.org/10.1016/j.gca.2020.03.027.
(34) Girard, C.; Leclerc, M.; Amyot, M. Photodemethylation of Methylmercury in Eastern Canadian Arctic Thaw Pond and Lake Ecosystems. *Environ. Sci. Technol.* **2016**, *50* (7), 3511–3520. https://doi.org/10.1021/acs.est.5b04921.
(35) Klapstein, S. J.; Ziegler, S. E.; O'Driscoll, N. J. Methylmercury Photodemethylation Is Inhibited in Lakes with High Dissolved Organic Matter. *Environ. Pollut.* **2018**, *232*, 392–401. https://doi.org/10.1016/j.envpol.2017.09.049.
(36) Zhang, T.; Hsu-Kim, H. Photolytic Degradation of Methylmercury Enhanced by Binding to Natural Organic Ligands. *Nat. Geosci.* **2010**, *3* (7), 473–476. https://doi.org/10.1038/ngeo892.
(37) Fernández-Gómez, C.; Drott, A.; Björn, E.; Díez, S.; Bayona, J. M.; Tesfalidet, S.; Lindfors, A.; Skyllberg, U. Towards Universal Wavelength-Specific Photodegradation Rate Constants for Methyl Mercury in Humic Waters, Exemplified by a Boreal Lake-Wetland Gradient. *Environ. Sci. Technol.* **2013**, *47* (12), 6279–6287. https://doi.org/10.1021/es400373s.
(38) Jeremiason, J. D.; Portner, J. C.; Aiken, G. R.; Hiranaka, A. J.; Dvorak, M. T.; Tran, K. T.; Latch, D. E. Photoreduction of Hg(II) and Photodemethylation of Methylmercury: The Key Role of Thiol Sites on Dissolved Organic Matter. *Environ. Sci.: Processes Impacts* **2015**, *17* (11), 1892–1903. https://doi.org/10.1039/C5EM00305A.
(39) Qian, Y.; Yin, X.; Lin, H.; Rao, B.; Brooks, S. C.; Liang, L.; Gu, B. Why Dissolved Organic Matter Enhances Photodegradation of Methylmercury. *Environ. Sci. Technol. Lett.* **2014**, *1* (10), 426–431. https://doi.org/10.1021/ez500254z.
(40) Zhang, X.; Li, Y.; Feng, G.; Tai, C.; Yin, Y.; Cai, Y.; Liu, J. Probing the DOM-Mediated Photodegradation of Methylmercury by Using Organic Ligands with Different Molecular Structures as the DOM Model. *Water Res.* **2018**, *138*, 264–271. https://doi.org/10.1016/j.watres.2018.03.055.
(41) Kim, M.-K.; Zoh, K.-D. Effects of Natural Water Constituents on the Photo-Decomposition of Methylmercury and the Role of Hydroxyl Radical. *Sci. Total Environ.* **2013**, *449*, 95–101. https://doi.org/10.1016/j.scitotenv.2013.01.039.
(42) Kim, M.-K.; Won, A.-Y.; Zoh, K.-D. Effects of Molecular Size Fraction of DOM on Photodegradation of Aqueous Methylmercury. *Chemosphere* **2017**, *174*, 739–746. https://doi.org/10.1016/j.chemosphere.2017.02.033.
(43) Fleck, J. A.; Gill, G.; Bergamaschi, B. A.; Kraus, T. E. C.; Downing, B. D.; Alpers, C. N. Concurrent Photolytic Degradation of Aqueous Methylmercury and Dissolved Organic Matter. *Science of The Total Environment* **2014**, *484*, 263–275. https://doi.org/10.1016/j.scitotenv.2013.03.107.
(44) Soerensen, A. L.; Schartup, A. T.; Skrobonja, A.; Bouchet, S.; Amouroux, D.; Liem-Nguyen, V.; Björn, E. Deciphering the Role of Water Column Redoxclines on Methylmercury Cycling Using Speciation Modeling and Observations From the Baltic Sea. *Global Biogeochem. Cycles* **2018**, *32* (10), 1498–1513. https://doi.org/10.1029/2018GB005942.
(45) Soerensen, Anne. L.; Schartup, A. T.; Gustafsson, E.; Gustafsson, B. G.; Undeman, E.; Björn, E. Eutrophication Increases Phytoplankton Methylmercury Concentrations in a Coastal Sea—A Baltic Sea Case Study. *Environmental Science & Technology* **2016**, *50* (21), 11787–11796. https://doi.org/10.1021/acs.est.6b02717.
(46) Soerensen, A. L.; Schartup, A. T.; Skrobonja, A.; Björn, E. Organic Matter Drives High Interannual Variability in Methylmercury Concentrations in a Subarctic Coastal Sea. *Environmental Pollution* **2017**, *229*, 531–538. https://doi.org/10.1016/j.envpol.2017.06.008.
(47) Soerensen, A. L.; Faxneld, S. *The Swedish National Monitoring Programme for Contaminants in Marine Biota (until 2019 Year's Data) - Temporal Trends and Spatial Variations*; Stockholm, 2020.

(48) Post, D. M.; Layman, C. A.; Arrington, D. A.; Takimoto, G.; Quattrochi, J.; Montaña, C. G. Getting to the Fat of the Matter: Models, Methods and Assumptions for Dealing with Lipids in Stable Isotope Analyses. *Oecologia* **2007**, *152* (1), 179–189.
(49) Aro, E. *A Review of Fish Migration Patterns in the Baltic*; 190; 1989; pp 72–96.
(50) Hansson, S.; Hobbie, J. E.; Elmgren, R.; Larsson, U.; Fry, B.; Johansson, S. The Stable Nitrogen Isotope Ratio as a Marker of Food-Web Interactions and Fish Migration. *Ecology* **1997**, *78* (7), 2249–2257. https://doi.org/10.1890/0012-9658(1997)078[2249:TSNIRA]2.0.CO;2.
(51) Karlsson, A.; Danielsson, S.; Ek, C.; Faxneld, S.; Nyberg, E.; Pütz Winkens, K. *Long-term changes in stable carbon and nitrogen isotopes in Blue mussels from Kvädöfjärden, Baltic Proper (1981-2017), and spatial comparisons of the isotope composition in Blue mussel and the Baltic clam from 13 stations along the Swedish coast (2015-2017)*; Stockholms Universitet, 2019.
(52) Seidel, M.; Manecki, M.; Herlemann, D. P. R.; Deutsch, B.; Schulz-Bull, D.; Jürgens, K.; Dittmar, T. Composition and Transformation of Dissolved Organic Matter in the Baltic Sea. *Frontiers in Earth Science* **2017**, *5*. https://doi.org/10.3389/feart.2017.00031.
(53) Josefsson, S. *Contaminants in Swedish Offshore Sediments 2003–2021. Results from the National Environmental Monitoring Programme.*; Swedish Environmental Protection Agency: Uppsala: Geological Survey of Sweden (SGU), 2022; p 103.
(54) Monperrus, M.; Tessier, E.; Veschambre, S.; Amouroux, D.; Donard, O. Yan. *Anal. Bioanal. Chem.* **2005**, *381* (4), 854–862.
(55) Jonsson, S.; Skyllberg, U.; Nilsson, M. B.; Lundberg, E.; Andersson, A.; Björn, E. Differentiated Availability of Geochemical Mercury Pools Controls Methylmercury Levels in Estuarine Sediment and Biota. *Nature Communications* **2014**, *5*, 4624. https://doi.org/10.1038/ncomms5624.
(56) Bérail, S.; Cavalheiro, J.; Tessier, E.; Barre, J. P. G.; Pedrero, Z.; Donard, O. F. X.; Amouroux, D. Determination of Total Hg Isotopic Composition at Ultra-Trace Levels by on Line Cold Vapor Generation and Dual Gold-Amalgamation Coupled to MC-ICP-MS. *J. Anal. At. Spectrom.* **2017**, *32* (2), 373–384. https://doi.org/10.1039/C6JA00375C.
(57) Blum, J. D.; Johnson, M. W. Recent Developments in Mercury Stable Isotope Analysis. *Rev Mineral Geochem* **2017**, *82* (1), 733–757. https://doi.org/10.2138/rmg.2017.82.17.
(58) Guédron, S.; Point, D.; Acha, D.; Bouchet, S.; Baya, P. A.; Tessier, E.; Monperrus, M.; Molina, C. I.; Groleau, A.; Chauvaud, L.; Thebault, J.; Amice, E.; Alanoca, L.; Duwig, C.; Uzu, G.; Lazarro, X.; Bertrand, A.; Bertrand, S.; Barbraud, C.; Delord, K.; Gibon, F. M.; Ibanez, C.; Flores, M.; Fernandez Saavedra, P.; Ezpinoza, M. E.; Heredia, C.; Rocha, F.; Zepita, C.; Amouroux, D. Mercury Contamination Level and Speciation Inventory in Lakes Titicaca & Uru-Uru (Bolivia): Current Status and Future Trends. *Environ. Pollut.* **2017**, *231*, 262–270. https://doi.org/10.1016/j.envpol.2017.08.009.
(59) Fitzgerald, W. F.; Lamborg, C. H.; Hammerschmidt, C. R. Marine Biogeochemical Cycling of Mercury. *Chem. Rev.* **2007**, *107* (2), 641–662.
(60) Leipe, T.; Moros, M.; Kotilainen, A.; Vallius, H.; Kabel, K.; Endler, M.; Kowalski, N. Mercury in Baltic Sea Sediments—Natural Background and Anthropogenic Impact. *Chemie der Erde - Geochemistry* **2013**, *73* (3), 249–259. https://doi.org/10.1016/j.chemer.2013.06.005.
(61) Kwasigroch, U.; Bełdowska, M.; Jędruch, A.; Łukawska-Matuszewska, K. Distribution and Bioavailability of Mercury in the Surface Sediments of the Baltic Sea. *Environ Sci Pollut Res* **2021**. https://doi.org/10.1007/s11356-021-13023-4.
(62) Gehrke, G. E. Mercury Cycling in the Marine Environment: Insights from Hg Stable Isotopes, 2011.
(63) Sun, R.; Streets, D. G.; Horowitz, H. M.; Amos, H. M.; Liu, G.; Perrot, V.; Toutain, J.-P.; Hintelmann, H.; Sunderland, E. M.; Sonke, J. E. Historical (1850–2010) Mercury Stable Isotope Inventory from Anthropogenic Sources to the Atmosphere. *Elementa: Science of the Anthropocene* **2016**, *4*, 000091. https://doi.org/10.12952/journal.elementa.000091.
(64) Jiskra, M.; Wiederhold, J. G.; Skyllberg, U.; Kronberg, R.-M.; Hajdas, I.; Kretzschmar, R. Mercury Deposition and Re-Emission Pathways in Boreal Forest Soils Investigated with Hg Isotope

Signatures. *Environ. Sci. Technol.* **2015**, *49* (12), 7188–7196. https://doi.org/10.1021/acs.est.5b00742.
(65) Demers, J. D.; Blum, J. D.; Zak, D. R. Mercury Isotopes in a Forested Ecosystem: Implications for Air-Surface Exchange Dynamics and the Global Mercury Cycle: MERCURY ISOTOPES IN A FORESTED ECOSYSTEM. *Global Biogeochem. Cycles* **2013**, *27* (1), 222–238. https://doi.org/10.1002/gbc.20021.
(66) Jiskra, M.; Wiederhold, J. G.; Skyllberg, U.; Kronberg, R.-M.; Kretzschmar, R. Source Tracing of Natural Organic Matter Bound Mercury in Boreal Forest Runoff with Mercury Stable Isotopes. *Environ. Sci.: Processes Impacts* **2017**, *19* (10), 1235–1248. https://doi.org/10.1039/C7EM00245A.
(67) Rose, C. H.; Ghosh, S.; Blum, J. D.; Bergquist, B. A. Effects of Ultraviolet Radiation on Mercury Isotope Fractionation during Photo-Reduction for Inorganic and Organic Mercury Species. *Chem. Geol.* **2015**, *405*, 102–111. https://doi.org/10.1016/j.chemgeo.2015.02.025.
(68) Sonke, J. E.; Schäfer, J.; Chmeleff, J.; Audry, S.; Blanc, G.; Dupré, B. Sedimentary Mercury Stable Isotope Records of Atmospheric and Riverine Pollution from Two Major European Heavy Metal Refineries. *Chemical Geology* **2010**, *279* (3), 90–100. https://doi.org/10.1016/j.chemgeo.2010.09.017.
(69) Meng, M.; Sun, R.; Liu, H.; Yu, B.; Yin, Y.; Hu, L.; Chen, J.; Shi, J.; Jiang, G. Mercury Isotope Variations within the Marine Food Web of Chinese Bohai Sea: Implications for Mercury Sources and Biogeochemical Cycling. *Journal of Hazardous Materials* **2020**, *384*, 121379. https://doi.org/10.1016/j.jhazmat.2019.121379.
(70) Nfon, E.; Cousins, I. T.; Järvinen, O.; Mukherjee, A. B.; Verta, M.; Broman, D. Trophodynamics of Mercury and Other Trace Elements in a Pelagic Food Chain from the Baltic Sea. *Science of The Total Environment* **2009**, *407* (24), 6267–6274. https://doi.org/10.1016/j.scitotenv.2009.08.032.
(71) Funk, S.; Frelat, R.; Möllmann, C.; Temming, A.; Krumme, U. The Forgotten Feeding Ground: Patterns in Seasonal and Depth-specific Food Intake of Adult Cod *GADUS MORHUA* in the Western Baltic Sea. *J Fish Biol* **2021**, *98* (3), 707–722. https://doi.org/10.1111/jfb.14615.
(72) Amyot, M.; Mierle, G.; Lean, D.; McQueen, D. J. Effect of Solar Radiation on the Formation of Dissolved Gaseous Mercury in Temperate Lakes. *Geochim. Cosmochim. Acta* **1997**, *61* (5), 975–987.
(73) Lepak, R. F.; Janssen, S. E.; Yin, R.; Krabbenhoft, D. P.; Ogorek, J. M.; DeWild, J. F.; Tate, M. T.; Holsen, T. M.; Hurley, J. P. Factors Affecting Mercury Stable Isotopic Distribution in Piscivorous Fish of the Laurentian Great Lakes. *Environ. Sci. Technol.* **2018**, *52* (5), 2768–2776. https://doi.org/10.1021/acs.est.7b06120.
(74) Sackett, D. K.; Drazen, J. C.; Popp, B. N.; Choy, C. A.; Blum, J. D.; Johnson, M. W. Carbon, Nitrogen, and Mercury Isotope Evidence for the Biogeochemical History of Mercury in Hawaiian Marine Bottomfish. *Environ. Sci. Technol.* **2017**, *51* (23), 13976–13984. https://doi.org/10.1021/acs.est.7b04893.
(75) Motta, L. C.; Blum, J. D.; Johnson, M. W.; Umhau, B. P.; Popp, B. N.; Washburn, S. J.; Drazen, J. C.; Benitez-Nelson, C. R.; Hannides, C. C. S.; Close, H. G.; Lamborg, C. H. Mercury Cycling in the North Pacific Subtropical Gyre as Revealed by Mercury Stable Isotope Ratios. *Global Biogeochem. Cycles* **2019**, *33* (6), 777–794. https://doi.org/10.1029/2018GB006057.
(76) Perrot, V.; Pastukhov, M. V.; Epov, V. N.; Husted, S.; Donard, O. F. X.; Amouroux, D. Higher Mass-Independent Isotope Fractionation of Methylmercury in the Pelagic Food Web of Lake Baikal (Russia). *Environ. Sci. Technol.* **2012**, *46* (11), 5902–5911. https://doi.org/10.1021/es204572g.
(77) Štrok, M.; Hintelmann, H.; Dimock, B. Development of Pre-Concentration Procedure for the Determination of Hg Isotope Ratios in Seawater Samples. *Anal. Chim. Acta* **2014**, *851*, 57–63. https://doi.org/10.1016/j.aca.2014.09.005.

(78) Štrok, M.; Baya, P. A.; Hintelmann, H. The Mercury Isotope Composition of Arctic Coastal Seawater. *Comptes Rendus Geoscience* **2015**, *347* (7), 368–376. https://doi.org/10.1016/j.crte.2015.04.001.
(79) Sherman, L. S.; Blum, J. D.; Keeler, G. J.; Demers, J. D.; Dvonch, J. T. Investigation of Local Mercury Deposition from a Coal-Fired Power Plant Using Mercury Isotopes. *Environ. Sci. Technol.* **2012**, *46* (1), 382–390. https://doi.org/10.1021/es202793c.
(80) Enrico, M.; Roux, G. L.; Marusczak, N.; Heimbürger, L.-E.; Claustres, A.; Fu, X.; Sun, R.; Sonke, J. E. Atmospheric Mercury Transfer to Peat Bogs Dominated by Gaseous Elemental Mercury Dry Deposition. *Environ. Sci. Technol.* **2016**, *50* (5), 2405–2412. https://doi.org/10.1021/acs.est.5b06058.
(81) Gratz, L. E.; Keeler, G. J.; Blum, J. D.; Sherman, L. S. Isotopic Composition and Fractionation of Mercury in Great Lakes Precipitation and Ambient Air. *Environ. Sci. Technol.* **2010**, *44* (20), 7764–7770. https://doi.org/10.1021/es100383w.
(82) Wang, Z.; Chen, J.; Feng, X.; Hintelmann, H.; Yuan, S.; Cai, H.; Huang, Q.; Wang, S.; Wang, F. Mass-Dependent and Mass-Independent Fractionation of Mercury Isotopes in Precipitation from Guiyang, SW China. *Comptes Rendus Geoscience* **2015**, *347* (7–8), 358–367. https://doi.org/10.1016/j.crte.2015.02.006.
(83) Rolison, J. M.; Landing, W. M.; Luke, W.; Cohen, M.; Salters, V. J. M. Isotopic Composition of Species-Specific Atmospheric Hg in a Coastal Environment. *Chemical Geology* **2013**, *336*, 37–49. https://doi.org/10.1016/j.chemgeo.2012.10.007.
(84) Fu, X.; Zhang, H.; Feng, X.; Tan, Q.; Ming, L.; Liu, C.; Zhang, L. Domestic and Transboundary Sources of Atmospheric Particulate Bound Mercury in Remote Areas of China: Evidence from Mercury Isotopes. *Environ. Sci. Technol.* **2019**, *53* (4), 1947–1957. https://doi.org/10.1021/acs.est.8b06736.
(85) Cai, H.; Chen, J. Mass-Independent Fractionation of Even Mercury Isotopes. *Science Bulletin* **2016**, *61* (2), 116–124. https://doi.org/10.1007/s11434-015-0968-8.
(86) Arheimer, B.; Donnelly, C.; Lindström, G. Regulation of Snow-Fed Rivers Affects Flow Regimes More than Climate Change. *Nat Commun* **2017**, *8* (1), 62. https://doi.org/10.1038/s41467-017-00092-8.
(87) Tsui, M. T.-K.; Blum, J. D.; Finlay, J. C.; Balogh, S. J.; Nollet, Y. H.; Palen, W. J.; Power, M. E. Variation in Terrestrial and Aquatic Sources of Methylmercury in Stream Predators as Revealed by Stable Mercury Isotopes. *Environ. Sci. Technol.* **2014**, *48* (17), 10128–10135. https://doi.org/10.1021/es500517s.
(88) Hüssy, K.; Albertsen, C. M.; Hemmer-Hansen, J.; Vinther, M.; Serre, S. H.; Thomsen, T. B.; Eero, M. Where Do You Come from, Where Do You Go: Early Life Stage Drift and Migrations of Cod Inferred from Otolith Microchemistry and Genetic Population Assignment. *Can. J. Fish. Aquat. Sci.* **2022**, *79* (2), 300–313. https://doi.org/10.1139/cjfas-2020-0409.
(89) Masbou, J.; Sonke, J. E.; Amouroux, D.; Guillou, G.; Becker, P. R.; Point, D. Hg-Stable Isotope Variations in Marine Top Predators of the Western Arctic Ocean. *ACS Earth Space Chem.* **2018**, *2* (5), 479–490. https://doi.org/10.1021/acsearthspacechem.8b00017.
(90) Xu, X.; Zhang, Q.; Wang, W.-X. Linking Mercury, Carbon, and Nitrogen Stable Isotopes in Tibetan Biota: Implications for Using Mercury Stable Isotopes as Source Tracers. *Sci Rep* **2016**, *6* (1), 25394. https://doi.org/10.1038/srep25394.
(91) Hjerne, O.; Hajdu, S.; Larsson, U.; Downing, A. S.; Winder, M. Climate Driven Changes in Timing, Composition and Magnitude of the Baltic Sea Phytoplankton Spring Bloom. *Frontiers in Marine Science* **2019**, *6*.
(92) Point, D.; Sonke, J. E.; Day, R. D.; Roseneau, D. G.; Hobson, K. A.; Vander Pol, S. S.; Moors, A. J.; Pugh, R. S.; Donard, O. F. X.; Becker, P. R. Methylmercury Photodegradation Influenced by Sea-Ice Cover in Arctic Marine Ecosystems. *Nature Geoscience* **2011**, *4* (3), 188–194. https://doi.org/10.1038/ngeo1049.
(93) https://en.ilmatieteenlaitos.fi/icestatistics. Sea ice statistics - Finnish Meteorological Institute https://en.ilmatieteenlaitos.fi/icestatistics (accessed 2023 -04 -11).

(94) Stock, A. Satellite Mapping of Baltic Sea Secchi Depth with Multiple Regression Models. *International Journal of Applied Earth Observation and Geoinformation* **2015**, *40*, 55–64. https://doi.org/10.1016/j.jag.2015.04.002.
(95) Deutsch, B.; Alling, V.; Humborg, C.; Korth, F.; Mörth, C. M. Tracing Inputs of Terrestrial High Molecular Weight Dissolved Organic Matter within the Baltic Sea Ecosystem. *Biogeosciences* **2012**, *9* (11), 4465–4475. https://doi.org/10.5194/bg-9-4465-2012.

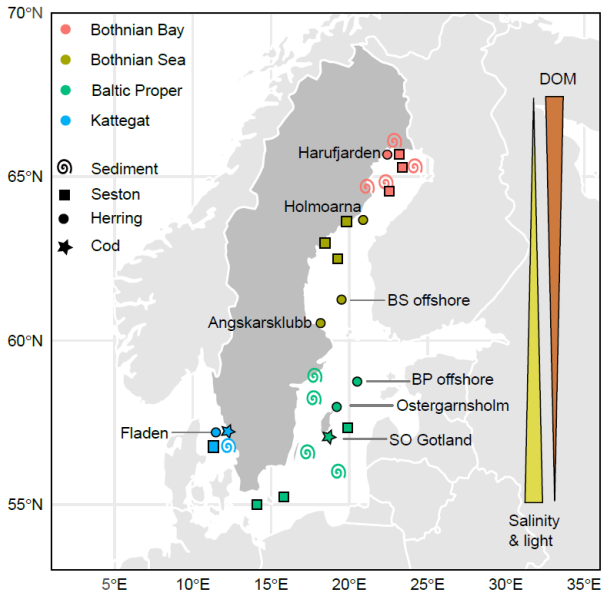

719

720

721 **Figure 1:** Map of the Baltic Sea with the various types of samples analyzed and their location. Specific sampling
722 stations are indicated for seston and fishes while several sediment samples were collected at each sediment area
723 indicated. There are several latitudinal gradients across the various basins with increases in salinity and light
724 irradiation, and decreases in concentration and terrestrial fraction of DOM, from the Bothnian Bay to the Kattegatt.

725

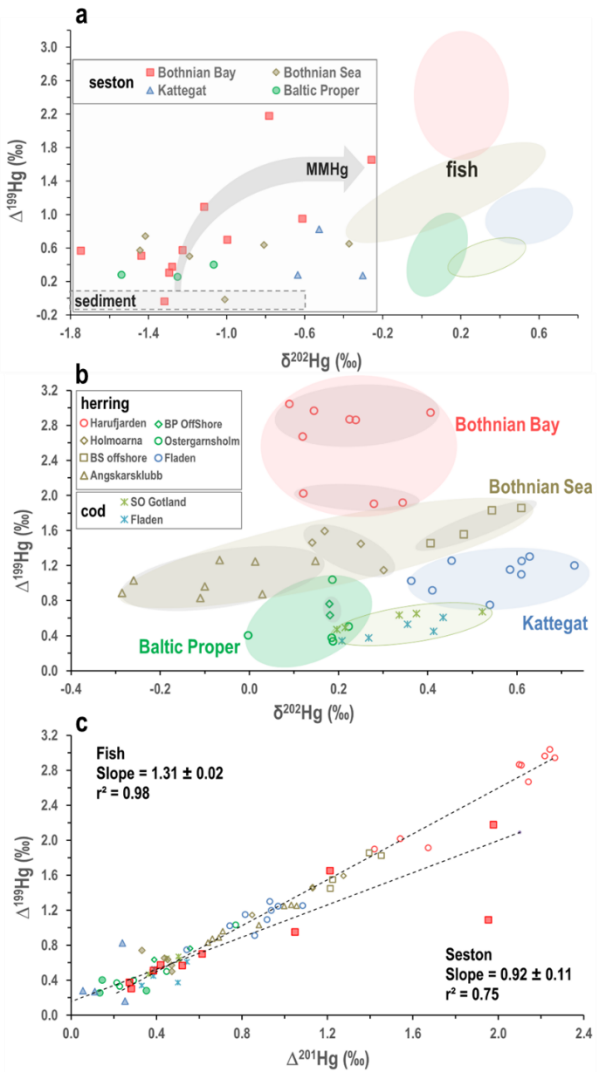

Figure 2: (a) Δ^{199}Hg versus δ^{202}Hg in seston (contours of sediments and fish are given for indication); (b) Δ^{199}Hg versus δ^{202}Hg in fish samples according to their basins, stations and fish species; (c) Δ^{199}Hg versus Δ^{201}Hg in fish and seston samples.

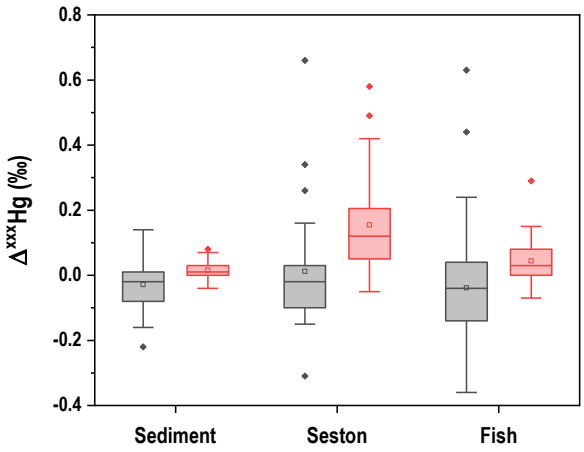

732

733

734 **Figure 3:** Distribution of Δ^{204}Hg (grey boxes) and Δ^{200}Hg (red boxes) in sediment, seston and fish samples.

735

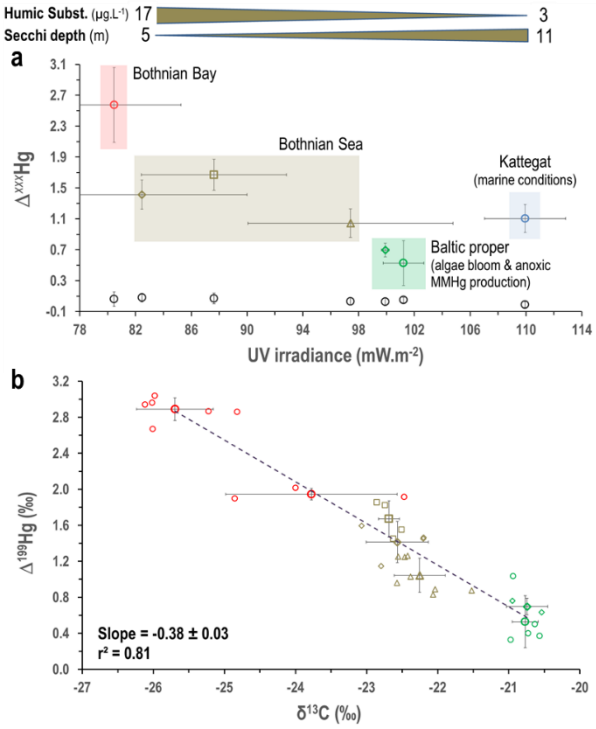

736

737

738 **Figure 4:** (a) Δ^{199}Hg (color coded) and their corresponding Δ^{200}Hg values (black, open circles) in herrings from
739 the various basins of the Baltic Sea versus the average UV irradiance; (b) Δ^{199}Hg in herrings from the various
740 basins (same color coding as in panel a) versus δ^{13}C.